catalysts

MDPI

Article

Analysis of Reaction Conditions in Palmitic Acid Deoxygenation for Fuel Production

Karoline K. Ferreira [1,2], Lucília S. Ribeiro [1,2,*] and Manuel Fernando R. Pereira [1,2]

[1] LSRE-LCM—Laboratory of Separation and Reaction Engineering-Laboratory of Catalysis and Materials, Faculty of Engineering, University of Porto, Rua Dr. Roberto Frias, 4200-465 Porto, Portugal; up202103294@edu.fe.up.pt (K.K.F.); fpereira@fe.up.pt (M.F.R.P.)

[2] ALiCE—Associate Laboratory in Chemical Engineering, Faculty of Engineering, University of Porto, Rua Dr. Roberto Frias, 4200-465 Porto, Portugal

* Correspondence: lucilia@fe.up.pt; Tel.: +351-220-414-922

Abstract: The development of effective catalytic systems for deoxygenation reactions is critical to the conversion of renewable feedstocks into sustainable fuels. In this work, the influence of various reaction parameters on the conversion of palmitic acid into alkanes, such as temperature, stirring rate, reaction time, H_2 pressure, amount of catalyst and substrate concentration was evaluated using the commercial Co-Mo/Al_2O_3 catalyst. In parallel, bimetallic Co-Mo catalysts supported on carbon nanotubes (CNTs) were prepared and characterized using various techniques, and their catalytic performance was assessed under the optimized conditions. The results showed that palmitic acid can be efficiently converted at 350 °C for 6 h at 30 bar H_2 pressure, stirring at 150 rpm and using 0.25 g of catalyst and 0.50 g of palmitic acid in 50 mL of n-decane. Under these conditions, a complete substrate conversion and yields of 89.4 and 4.8% of C_{16} and C_{15} were achieved. In addition, Co-Mo/CNT_{ox} presented a similar catalytic performance as the commercial one, with a final result of 90.9% yield in C_{16}. These findings point out the potential of using Co-Mo/CNT_{ox} as a competitive alternative to liquid fuel production.

Keywords: palmitic acid; deoxygenation; optimization; Co-Mo catalysts

Citation: Ferreira, K.K.; Ribeiro, L.S.; Pereira, M.F.R. Analysis of Reaction Conditions in Palmitic Acid Deoxygenation for Fuel Production. *Catalysts* **2024**, *14*, 853. https://doi.org/10.3390/catal14120853

Academic Editor: Sergio Nogales Delgado

Received: 6 November 2024
Revised: 21 November 2024
Accepted: 22 November 2024
Published: 24 November 2024

1. Introduction

The transport sector has a great influence on the global dynamics of societies, directly contributing to the mobility of people, products and services. Although essential, transportation contributes to the growth of greenhouse gas (GHG) emissions and other pollutants as a result of the combustion of petrochemical-based jet fuel. Global transportation-related CO_2 emissions increased by 250 Mt from 2021 to 2022 [1]. To overcome this challenge, the growing demand for clean and renewable energy sources has motivated substantial study into the development of advanced biofuels as alternatives to traditional fossil fuels.

Due to its strict quality standards and the urgency to mitigate carbon emissions, the production of alternative liquid fuels, essential across various sectors, presents a distinctive challenge. In the pursuit of eco-friendly alternatives, the utilization of lipidic feedstock derived from biomass holds significant potential, particularly in the production of these fuels [2]. For example, microalgae bio-oil, oilseeds, vegetable oils and waste cooking oils contain high levels of fatty acids with carbon chains in the range of C_{14}–C_{22}, the desired carbon number for liquid fuel hydrocarbons [3]. Free fatty acids can be obtained during the refining of vegetable oils, by steam refining or by the hydrolysis of lipid matrices (e.g., vegetable oils and animal fats) [4]. For example, palmitic acid ($C_{16}H_{32}O_2$) is the simplest saturated chain fatty acid and is abundant in lipid sources. It is currently derived from the alkaline hydrolysis of palm oil [5].

Even though using this biomass has several benefits, it cannot be used as a drop-in fuel, which is a liquid biohydrocarbon functionally comparable to petrochemical-based

fuels and completely compatible with the infrastructure already in place at petroleum refineries, including the engines and turbines where they are employed [6]. The high content of oxygenated compounds present in lipid biomass brings some disadvantages to its physicochemical properties, such as high acidity, low chemical instability, high viscosity and low heating value [7–9].

With the aim of improving these physical and chemical properties, some studies involving the deoxygenation of lipid biomass model molecules, such as fatty acids, have been carried out [10–15]. Considering a fatty acid, deoxygenation reaction occurs through a hydrotreating catalyst via three different reaction pathways, as described in equations 1, 2 and 3 [15]:

$$\text{Hydrodecarbonylation (HDC): R-COOH} + H_2 \rightarrow \text{R-H} + CO + H_2O \quad (1)$$

$$\text{Decarboxylation (DCX): R-COOH} \rightarrow \text{R-H} + CO_2 \quad (2)$$

$$\text{Hydrodeoxygenation (HDO): R-COOH} + 3H_2 \rightarrow \text{R-CH}_3 + 2H_2O \quad (3)$$

In an HDO reaction, oxygen atoms can be removed by forming two water molecules via exothermic hydrodeoxygenation, which requires three moles of hydrogen per one fatty acid molecule. Hence, n-alkane with the same number of carbon atoms as the corresponding fatty acid is formed. In addition, HDO does not produce carbon monoxide (CO) or carbon dioxide (CO_2), as observed in HDC and DCX reactions, which is attractive regarding environmental issues [16,17].

In the petrochemical industry, bimetallic CoMo and NiMo catalysts supported on oxides such as γ-Al_2O_3 are frequently employed to remove heteroatoms in hydrotreating units [18]. Studies have examined the deoxygenation of fatty acids into n-alkanes using mono- and bimetallic Co and Mo catalysts supported on zeolites extensively in recent years [12,15,19]. These materials have acidic active sites that enhance the final chemical composition of jet fuel by producing iso-alkanes, which in turn enhances its cold properties. However, zeolites are unstable and derived from inorganic sources. The effectiveness of carbon-based materials like carbon nanotubes (CNTs) as catalyst supports has not been extensively studied. The high thermal and chemical stability of these materials; their high porosity, which facilitates the diffusion of reactants to active sites; and their ease of modification of the surface, which changes its chemical composition and textural properties, stand out among their many advantages [20].

With the increased use of carbon-based materials as catalysts, new approaches have been tested by many researchers in recent years. Zhong et al. [21] assessed the deoxygenation of stearic acid – $C_{18}H_{36}O_2$ (vegetable oil model compound) over a carbon-coated bimetallic FeNi catalyst. After 3 h of reaction at 330 °C, the authors obtained about 77% of heptadecane, and a small fraction of oxygenated compounds and jet fuel hydrocarbons. Liu et al. [22] investigated the deoxygenation of palmitic acid as a model compound of microalgae bio-oils using Pt/C as a catalyst under hydrothermal conditions and formic acid for in-situ H_2 generation. A conversion of 67.7% and a yield of 42.2% in pentadecane was achieved after 90 min of reaction at 370 °C. Although the short reaction time and the possibility of in situ H_2 production are advantages, the high cost associated with the use of noble metals makes the catalytic process more expensive. In the following years, Lin et al. [23] studied non-noble metals supported on activated carbon (AC) in the HDO of palmitic acid. The results showed that pre-reduced Ni/AC exhibited high selectivity for pentadecane and hexadecanol, whereas commercial Ru/AC was more selective for smaller alkanes. Although promising, most recent studies in this field focused on carbon-based materials with predominantly microporous structures. While these materials show excellent performance in applications with model compounds, their limited pore size may be a significant drawback when dealing with more complex feedstocks, such as bio-oil or waste cooking oil.

Taking into account the previously mentioned concepts, this study assessed the deoxygenation reactions of palmitic acid in detail, concentrating on the optimization of reaction

parameters using the commercial Co-Mo/Al_2O_3 catalyst, and its stability after many reaction cycles. Additionally, CoMo catalysts supported on CNTs with the same metal content as the commercial catalyst were synthesized and evaluated under the optimized conditions. Studies using CNT-based catalysts for deoxygenation reactions are scarce. Furthermore, studies comparing untreated and chemically modified CNTs with commercial catalysts are also uncommon in the literature.

2. Results and Discussion

2.1. Characterization Results

The reducibility of the prepared bimetallic catalysts was studied by temperature programmed reduction (TPR) and the resulting profiles can be found in the Supplementary Materials (Figure S1). According to the results, Co-Mo/CNT presented two broad peaks at 500 and 600 °C, whereas Co-Mo/CNT_{ox} showed a reduction peak at 500 °C. To prepare both catalysts under the same conditions, 600 °C was selected for the reduction and thermal treatment.

The elemental analysis and metal content of the catalyst and the supports are presented in Table 1. The metal loading of each synthesized carbon catalyst was selected based on the inductively coupled plasma-optical emission spectroscopy (ICP-OES) analysis of the Co-Mo/Al_2O_3. Therefore, each catalyst was prepared containing 2.5 wt.% of Co and 10.5 wt.% of Mo. The ICP-OES analysis confirmed the amount of metal impregnated into the support. The nominal Mo values for both catalysts were practically the same as the theoretical value. However, the percentages of Co obtained were slightly lower due to losses of the precursor in the impregnation step. The treatment of CNTs with nitric acid led to the introduction of oxygenated groups as the oxygen content in the sample increased from 1.78 to 4.38%. However, a similar amount of oxygen was observed in both bimetallic carbon catalysts. The temperature used in the reduction treatment (600 °C) led to a decomposition of most of the oxygenate compounds created on the CNT surface [24,25].

Table 1. Elemental analysis and metal content of the samples.

Samples	C (%) [1]	O (%) [1]	H (%) [1]	Co (%) [2]	Mo (%) [2]
CNT	89.75	1.78	0.36	-	-
CNT_{ox}	93.44	4.38	1.38	-	-
Co-Mo/CNT	69.47	8.92	0.55	1.4	10.0
Co-Mo/CNT_{ox}	76.37	9.21	0.64	1.4	10.3
Co-Mo/Al_2O_3	0.30	16.16	1.31	2.5	10.5

[1] Determined by elemental analysis. [2] Determined by ICP-OES.

The textural properties of the catalysts and the supports were determined by N_2 adsorption isotherms. As shown in Table 2, the Co-Mo/Al_2O_3 catalyst presents a specific surface area of 247 $m^2\ g^{-1}$ and a volume pore of 0.60 $cm^3\ g^{-1}$. On the other hand, carbon-based catalysts exhibit a higher pore volume compared with commercial catalysts. The CNT_{ox} sample has a higher S_{BET} than the original CNT—262 and 229 $m^2\ g^{-1}$, respectively. This characteristic is due to the oxidative treatment with HNO_3 performed on the material, opening some of the edges of the CNT and creating defects in the sidewalls. In addition, introducing oxygenated groups on the surface causes a slight reduction in the pore volume of CNT_{ox} when compared to the CNT [25]. The introduction of the metal phases into the supports caused a decrease in the area of both catalysts. There was also a reduction in the pore volume of Co-Mo/CNT_{ox} but no prominent decrease in the pore volume of Co-Mo/CNT. Aiming to investigate the acidity of the materials, the pH at the point of zero charge (pH_{PZC}) was measured (Table 2 and Figure S2). The results show an acid character in CNTs after the treatment with HNO_3 due to the introduction of oxygenated groups. Even with the decrease in oxygen content observed in elemental analysis, the interaction of the metals with the support allowed the maintenance of acidic sites in the Co-Mo/CNT_{ox}

catalyst. On the other hand, the Co-Mo/CNT and Co-Mo/Al_2O_3 catalysts presented a more neutral chemical surface, with the commercial catalyst being the less acidic material.

Table 2. Textural properties and values of pH_{PZC} of the supports and catalysts.

Samples	S_{BET} ($m^2\ g^{-1}$)	S_{meso} ($m^2\ g^{-1}$)	V_{micro} ($cm^3\ g^{-1}$)	V_p [1] ($cm^3\ g^{-1}$)	pH_{PZC}
CNT	229	229	-	1.54	5.3
CNT_{ox}	262	262	-	1.44	2.4
Co-Mo/CNT	198	198	-	1.51	4.7
Co-Mo/CNT_{ox}	227	227	-	1.24	3.9
Co-Mo/Al_2O_3	247	247	-	0.60	5.5

[1] Pore volume calculated from the amount of N_2 adsorbed at $P/P_0 = 0.98$.

An X-ray diffraction (XRD) analysis (Figure 1) was also performed on the catalysts to investigate the crystallinity structures of the metals on the materials. Different peaks correlated to Mo and Co oxides were identified. In CNT catalysts, diffraction peaks were observed at 2θ = 26.0°, 37.1° and 53.5°, corresponding to the graphite structure of CNTs ([011]) and MoO_2 planes ([020] and [022]), respectively [9]. Peaks correlated to $Co_2Mo_3O_8$ were also detected in carbon-based catalysts (2θ = 17.9° [002], 19.9° [101], 25.3° [102] and 35.7° [200]) but were at a higher intensity in Co-Mo/CNT_{ox} [10,26]. The synthesized catalysts showed diffractograms with higher crystallinity compared to Co-Mo/Al_2O_3. Peaks correlated to the support γ-Al_2O_3 (2θ = 39.5° [111], 45.9° [200], 25.3° and 66.9° [220]) and MoO_3 (2θ = 46.2° [220] and 67.5° [400]) were found to overlap [27]. Moreover, peaks of MoO_2 (2θ = 37.1°) and hydrated $Co_2Mo_3O_8$ (2θ = 39.8° [204]) were also observed.

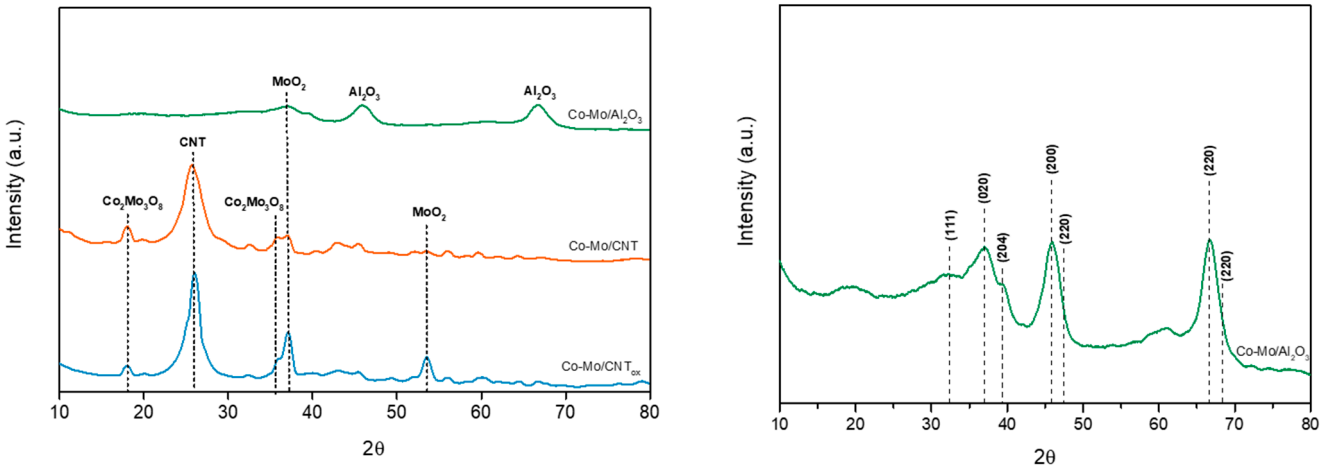

Figure 1. (**a**) XRD patterns of the catalysts; (**b**) enlarged diffractogram of Co-Mo/Al_2O_3.

2.2. Catalytic Conversion of Palmitic Acid

The study started with the assessment of the reaction temperature from 220 to 370 °C. As shown in Table 3, a substantial increase in the palmitic acid conversion was observed above 260 °C. Although the first alkanes started to form at 300 °C, the palmitic acid was completely converted only at 350 °C, reaching yields of C_{16} and C_{15} of 73.0% and 4.1%, respectively. Increasing the temperature to 370 °C did not improve the conversion and product yields; thus, 350 °C was selected for the following experiments. According to Li et al., the HDO reaction occurs firstly by hydrogenation of palmitic acid to hexadecanal and then to hexadecanol [19]. After these steps, the alcohol is dehydrated to the corresponding alkene and hydrogenated to form hexadecane. The dehydration step of hexadecanol

requires more activation energy; thus, increasing the temperature promotes the production of hexadecane significantly.

Table 3. Effect of temperature on palmitic acid conversion and product distribution.

T (°C)	*X* ± 2.8 (%)	Y_{C15} ± 0.3 (%)	Y_{C16} ± 5.3 (%)
220	0	0.0	0.0
260	32	0.0	0.0
300	46	0.7	13.6
325	78	1.4	24.6
350	100	4.1	73.0

Reaction conditions: palmitic acid (0.50 g), n-decane (50 mL), Co-Mo/Al_2O_3 (0.25 g), 220–370 °C, 40 bar H_2, 300 rpm, 4 h.

Subsequently, tests to evaluate the influence of the stirring rate were performed in the range of 150 to 700 rpm (Table 4). The particle distribution in the liquid phase was uniform inside the reactor, and a 100% palmitic acid conversion was achieved in all the experiments. No relevant change in the product distribution was observed at 150 rpm and above, indicating no external mass transfer limitations. According to the results, as the yield values in C_{15} and C_{16} were similar at all stirring rates, 150 rpm was used for the remaining tests.

Table 4. Influence of stirring rate on palmitic acid conversion and product distribution.

Stirring Rate (rpm)	*X* (%)	Y_{C15} ± 0.3 (%)	Y_{C16} ± 5.3 (%)
150	100	3.6	72.6
300	100	4.0	73.0
400	100	3.1	71.1
700	100	1.7	75.6

Reaction conditions: palmitic acid (0.50 g), n-decane (50 mL), Co-Mo/Al_2O_3 (0.25 g), 350 °C, 40 bar H_2, 150–700 rpm, 4 h.

The influence of the reaction time on the deoxygenation of palmitic acid with the Co-Mo/Al_2O_3 catalyst was also evaluated (Figure 2). In addition to the complete substrate conversion at 4 h, prolonging the reaction time to 6 h was sufficient to obtain a higher yield of C_{16} alkane (89.0%). Moreover, the C_{15} yield did not significantly change over time, indicating that the decarboxylation (DCX) and hydrodecarbonylation (HDC) reactions are insensitive to this parameter. A slight increase in the yield of C_{15} was observed from 4 to 8 h, raising its final value to 5.8%. Thus, 6 h was selected as the optimal reaction time for the subsequent reactions.

The effect of the catalyst amount was investigated by varying the Co-Mo/Al_2O_3 mass from 0.10 to 0.40 g. According to the results shown in Table 5, the palmitic acid conversion stayed the same (100%) in all experiments, achieving a C_{16} yield of around 89.0% using 0.25 and 0.40 g of the catalyst. A slight reduction in the C_{15} yield was seen with the increase in the catalyst mass in the reactor. Since the dehydration of the hexadecanol also requires acid sites, the HDO route is favored by improving the amount of catalyst, while the HDC and DCX routes are moderately suppressed. Regarding these results, since no significant difference was observed by raising the mass from 0.25 to 0.40 g, the following experiments were conducted using 0.25 g of the catalyst.

The amount of substrate was assessed by varying it from 0.25 to 0.75 g (Table 6). Increasing the amount of palmitic acid from 0.25 to 0.50 g slightly improved the C_{15} yield from 2.2 to 4.8%, while the C_{16} did not significantly change. On the other hand, raising the substrate to 0.75 g decreased the production of C_{15} and C_{16} to 1.6 and 72.1%, respectively. Regarding these results, in order to maintain the minimum catalyst–substrate ratio, the following experiments were performed using 0.50 g of the substrate.

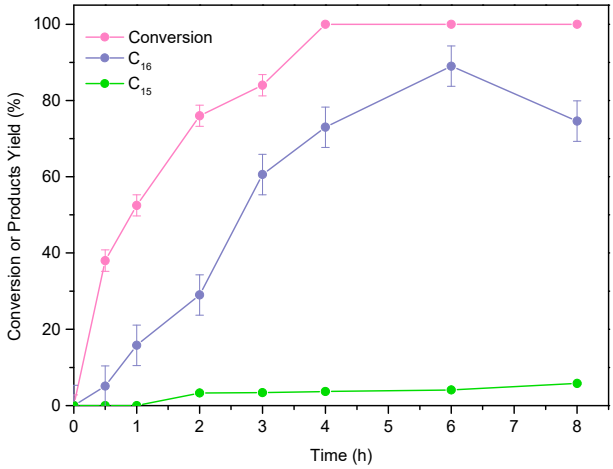

Figure 2. Influence of time on palmitic acid conversion and product yield. Reaction conditions: palmitic acid (0.50 g), n-decane (50 mL), Co-Mo/Al_2O_3 (0.25 g), 350 °C, 40 bar H_2, 150 rpm.

Table 5. Effect of the catalyst amount on palmitic acid conversion and product distribution.

$m_{catalyst}$ (g)	X (%)	$Y_{C15} \pm 0.3$ (%)	$Y_{C16} \pm 5.3$ (%)
0.10	100	6.0	55.8
0.25	100	4.8	89.0
0.40	100	3.6	89.9

Reaction conditions: palmitic acid (0.50 g), n-decane (50 mL), Co-Mo/Al_2O_3 (0.10–0.40 g), 350 °C, 40 150 rpm, 6 h bar H_2.

Table 6. Effect of the amount of substrate in the conversion and product distribution.

Palmitic Acid Amount (g)	X (%)	$Y_{C15} \pm 0.3$ (%)	$Y_{C16} \pm 5.3$ (%)
0.25	100	2.2	82.3
0.50	100	4.8	89.0
0.75	100	1.6	72.1

Reaction conditions: palmitic acid (0.25–0.75 g), n-decane (50 mL), Co-Mo/Al_2O_3 (0.25 g), 350 °C, 40 bar H_2, 150 rpm, 6 h.

Finally, the last parameter evaluated was the influence of hydrogen pressure. The results in Figure 3 show the conversion of palmitic acid and product yield using a pressure range from 20 to 40 bar. The substrate conversion remained at 100% in all the experiments. Regarding the product distribution, the C_{16} yield was improved from 22.7 to 89.4% when the pressure was increased from 20 to 30 bar, while raising the pressure to 40 bar did not affect the yield values. In higher-pressure conditions, the HDO route is favored since it requires a larger amount of hydrogen molecules than HDC. On the other hand, the production of C_{15} from the DCX route or aldehyde decarboxylation does not demand hydrogen [12,28]. In fact, throughout each test, hydrogen pressure had no effect on the C_{15} yield, showing that the DCX route was taken for the production of this alkane. Considering the above results, it can be concluded that 30 bar of H_2 is more suitable for the following reactions.

The stability of the Co-Mo/Al_2O_3 catalyst was also investigated, as shown in Figure S3, where six runs were performed under the same conditions. After each cycle, the catalyst was recovered by filtration and was properly washed and dried for the next catalytic run. No considerable decline in the catalyst activity was observed over all six consecutive runs, demonstrating the high stability of the commercial catalyst under the optimized conditions.

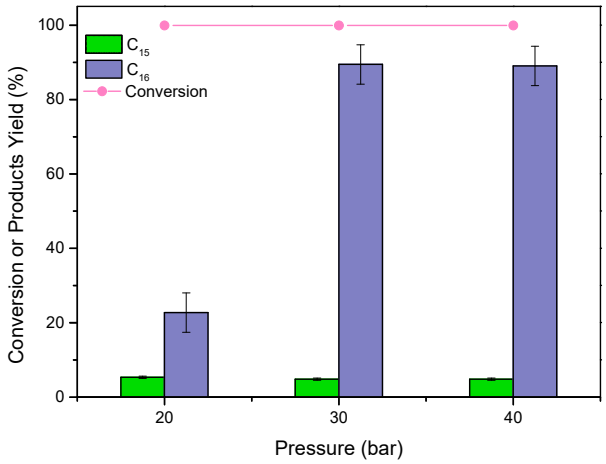

Figure 3. Effect of the hydrogen pressure on product yield. Reaction conditions: palmitic acid (0.50 g), n-decane (50 mL), Co-Mo/Al_2O_3 (0.25 g), 350 °C, 20–40 bar H_2, 150 rpm, 6 h.

In a further analysis, bimetallic Co-Mo catalysts supported on carbon nanotubes (Co-Mo/CNT and Co-Mo/CNT_{ox}) were tested under the optimized reaction conditions. Moreover, a blank experiment and reactions only with the supports were also performed to validate the catalysts' activity. The carbon-supported metal catalysts were shown to have excellent performance after 6 h of reaction with 60.4 and 90.9% of the C_{16} yield for Co-Mo/CNT and Co-Mo/CNT_{ox}, respectively (Table 7). Regarding the production of C_{15}, the yields were similar for both catalysts—10.5% for Co-Mo/CNT and 11.9% for Co-Mo/CNT_{ox}. These results show that, in addition to the DCX route, C_{15} is also produced by the decarbonylation of the intermediate aldehyde, increasing the yield of this alkane. This can be explained by the higher acidity shown in the CNT catalysts. The introduction of oxygenated groups on the surface of the CNT after its oxidation treatment was beneficial in enhancing the catalytic performance of the HDO reaction to the complete palmitic acid deoxygenation. Comparing the CNT_{ox} and Co-Mo/CNT_{ox} results, it is clear that the metallic phases were crucial to raising the C_{16} products and suppressing the HDC and DCX reactions. The lower acidity of the commercial catalyst and the higher Co content in the material may have contributed to a higher production of C_{16} compared to Co-Mo/CNT. On the other hand, the high presence of MoO_2 and Co and Mo oxides and the high acidity of the Co-Mo/CNT_{ox} catalyst provided similar performance to the commercial catalyst in terms of C_{16} production at the end of the 6 h reaction. Other studies assessed the deoxygenation of palmitic acid using CNT-based catalysts. These results are similar to those reported by Ding et al. [10], who achieved a high selectivity of 92.2% for C_{16} alkanes using a 5% MoO_2/CNT catalyst. Furthermore, after modifying the catalyst to include 1.5 % Co (1.5% Co-5% MoO_2/CNT), the selectivity remained excellent, reaching 89.3% for C_{16} alkanes [26]. On the other hand, studies performed by Cao et al. [12] and Shi et al. [15] demonstrated the effectiveness of zeolite-supported Co and Mo catalysts (ZSM-22), highlighting their ability to produce light alkanes and isomers. This behavior is attributed to the increased acidity of the zeolite support, which promotes additional cracking and isomerization reactions, enhancing the diversity of hydrocarbon products, and consequently decreasing the selectivity for C_{16} to about 15% in both studies.

To investigate the contribution of the metals separately, the reactions were carried out with Co/CNT and the physical mixture of Co/CNT and Mo/CNT. According to the results (Table S1), the reaction with Co/CNT provided 44.6% of C_{15} and 40.9% of C_{16}. However, in the reaction performed with the physical mixture of both monometallic catalysts (Co/CNT and Mo/CNT), a reduction in C_{15} to 39.2% and an improvement in C_{16} to 44.6% can be observed in addition to the production of smaller alkanes (dodecane, tridecane and tetradecane). These results show that the presence of the $Co_2Mo_3O_8$ alloy in the bimetallic catalysts observed by the XRD technique (Figure 1) contributes to a higher

yield of C_{16}, mostly favoring the HDO route compared to the metals individually supported on the CNTs.

Table 7. Palmitic acid conversion and product distribution.

Catalyst (g)	$X \pm 2.8$ (%)	$Y_{C15} \pm 0.3$ (%)	$Y_{C16} \pm 5.3$ (%)
Blank (no catalyst)	52	2.2	3.3
Al_2O_3	24	1.5	0.7
CNT	65	19.5	2.7
CNT_{ox}	77	48.0	24.0
Co-Mo/CNT	100	10.5	60.4
Co-Mo/CNT_{ox}	100	11.9	90.9
Co-Mo/Al_2O_3	100	4.8	89.0

Reaction conditions: palmitic acid (0.50 g), n-decane (50 mL), catalyst (0.25 g), 350 °C, 30 bar H_2, 150 rpm, 6 h.

3. Materials and Methods

3.1. Chemicals and Materials

Palmitic acid, multi-walled carbon nanotubes (CNTs) (Nanocyl-7000, purity of 90%) and n-decane (99%) were provided by Acro Organics (Waltham, MA, USA), Nanocyl (Sambreville, Belgium) and VWR ((Radnor, PA, USA), respectively. The metal precursors ammonium heptamolybdate (99.7%) and cobalt (II) nitrate hexahydrate (99%) were purchased from VWR and Sigma Aldrich (Darmstadt, Germany), respectively. Commercial Co-Mo/Al_2O_3 was acquired from Alfa Aesar (Waltham, MA, USA).

3.2. Catalysts Preparation

The following materials were used: (a) original CNTs and (b) CNT sample modified by an oxidation treatment with HNO_3 (7 mol L^{-1}) heated to the boiling temperature for 3 h. After that, the oxidized CNT (CNT_{ox}) was subsequently washed with distilled water until it was pH neutral, and then the material was dried at 110 °C for 24 h [25]. Bimetallic catalysts (nominal metal loadings of 2.5 and 10.5% of Co and Mo, respectively) were prepared by incipient wetness co-impregnation using an aqueous solution of the corresponding metallic precursors, added dropwise to each support material. After impregnation, the materials were dried overnight at 110 °C in an oven and then a thermal treatment was performed under N_2 flow for 3 h at 600 °C, followed by reduction under H_2 flow for 3 h at 600 °C. The appropriate reduction temperature was determined by TPR (Figure S1). The prepared catalysts were denoted as Co-Mo/CNT and Co-Mo/CNT_{ox}. Following the same procedure, the corresponding monometallic catalysts (2.5% Co and 10.5% Mo) were also prepared and denoted as Co/CNT and Mo/CNT.

3.3. Catalysts Characterization

The textural properties analysis of the supports and catalysts was established by N_2 adsorption isotherms at −196 °C. The samples were first degassed at 150 °C for 3 h under vacuum and the analyses were performed in a Quantachrome NOVA 4200e Surface Area and Pore Size analyzer (Anton Paar GmbH, Graz, Austria). Total specific surface areas were determined according to the Brunauer–Emmett–Teller method (S_{BET}), and the micropore volumes (V_{micro}) and mesopore surface areas (S_{meso}) were determined by the *t*-method. H_2-TPR profiles were obtained using a fully automated AMI-200 equipment (Altamira Instruments, PA, USA), submitted to a 10 °C min^{-1} heating to 900 °C under 5% (*v*/*v*) H_2 flow diluted in He. The powder XRD patterns of the catalysts were collected on a Philips X'Pert MPD diffractometer (Cu-Kα = 0.15406 nm, Malvern Panalytical, Almelo, The Netherlands). The diffracted intensity of Cu-Kα radiation was measured in the 2θ range between 10° and 100°. The cobalt and molybdenum loads present in each sample were obtained by ICP-OES using the ICPE-9000 spectrometer (Shimadzu, Kyoto, Japan). Elemental analysis (vario Micro Analysis CHNS and OXY cube analyser, Elementar Analysensysteme GmbH, Langenselbold, Germany) was performed to determine the amount of carbon, hydrogen

and oxygen present in the commercial catalyst and carbon materials. The pH at the point of zero charge (pH_{PZC}) was determined by measuring the pH level of the catalyst and supports in an aqueous solution before and after stirring for 24 h. For each dispersion, 25 mg of material was suspended in 25 mL of ultrapure water and the pH was adjusted between 2 and 12 with sodium hydroxide and/or hydrochloric acid.

3.4. Catalytic Experiments

The catalytic palmitic acid deoxygenation reactions were performed in a 100 mL stainless batch reactor (Parr Instruments, IL, USA, Mod HPHT 4598). A typical reaction was conducted as follows: palmitic acid (0.25–0.75 g), n-decane (50 mL) and catalyst (0.10–0.40 g) were loaded onto the reactor, which was then purged with H_2 at ambient temperature and then adjusted to the desired H_2 pressure (20–40 bar). Finally, the mixture was heated to the desired temperature (220–370 °C) under the required stirring rate (150–700 rpm) for 0.5–8 h. After adjusting the best reaction conditions, the stability of Co-Mo/Al_2O_3 and the Co-Mo/CNT and Co-Mo/CNT_{ox} catalytic performances were assessed.

The final liquid phase products were analyzed by a Dani GC-FID, model 1000 (Dani Instruments, Milan, Italy,) using a column TRB-5-RTX (30 m × 0.25 mm, 0.25 µm). The products detected were pentadecane (C_{15}) and hexadecane (C_{16}). Conversion of palmitic acid (X) and yield (Y_i) of each product i were calculated as indicated in equations 4 and 5, respectively.

$$X\ (\%) = \left(\frac{moles\ of\ converted\ palmitic\ acid}{moles\ of\ initial\ palmitic\ acid} \right) \times 100 \quad (4)$$

$$Y_i\ (\%) = \left(\frac{moles\ of\ product\ i}{moles\ of\ initial\ palmitic\ acid} \right) \times 100 \quad (5)$$

The experiments were carried out in triplicate and the standard deviations associated with the conversion and the yields of C_{15} and C_{16} were 2.8, 0.3 and 5.3%, respectively.

4. Conclusions

The reaction conditions were examined employing the commercial Co-Mo/Al_2O_3 catalyst to evaluate the deoxygenation pathways of palmitic acid. The production of C_{16} was at 89.0% under the conditions of 350 °C for 6 h at 30 bar H_2 pressure, stirring at 150 rpm and using 0.25 g of the catalyst and 0.50 g of palmitic acid in 50 mL of n-decane, indicating that the HDO route was favored. The Co and Mo catalysts supported on CNTs produced a greater amount of C_{15} under the optimized conditions, indicating that the DCX reaction was favored due to the greater acidity of these catalysts. Co-Mo/CNT_{ox} had a similar performance compared to the commercial catalyst, producing 90.9% of C_{16}, indicating that the higher acidity and the elevated presence of MoO_2 in its structure can not only favor C_{15} products but also C_{16} alkane. Further studies should focus on optimizing the Co-Mo/CNT_{ox} catalyst by determining the ideal metal phase proportions and adjusting temperature treatment conditions. This would improve the catalytic performance approaching the obtention of not only C_{15} and C_{16}, but also some other light alkanes hydrocarbons. Such information would provide the basis for conducting a comprehensive cost-benefit analysis of using Co-Mo/CNT_{ox} catalyst as an alternative material for advanced hydrocarbon synthesis in different liquid fuel ranges.

Supplementary Materials: The following supporting information can be downloaded at https://www.mdpi.com/article/10.3390/catal14120853/s1, Figure S1: TPR curves of the carbon-supported catalysts.; Figure S2: Curves of the pH at the point of zero charge (pH_{PZC}) for the catalysts and supports. Figure S3: Recyclability experiments. Figure S4: Products chromatogram of the recyclability reactions. Table S1: Palmitic acid conversion and product distribution using monometallic catalysts.

Author Contributions: Conceptualization, L.S.R. and M.F.R.P.; methodology, K.K.F., L.S.R. and M.F.R.P.; validation, K.K.F., L.S.R. and M.F.R.P.; formal analysis, K.K.F.; investigation, K.K.F., L.S.R. and M.F.R.P.; resources, M.F.R.P.; data curation, K.K.F.; writing—original draft preparation, K.K.F.;

writing—review and editing, K.K.F., L.S.R. and M.F.R.P.; supervision, L.S.R. and M.F.R.P.; funding acquisition, M.F.R.P. All authors have read and agreed to the published version of the manuscript.

Funding: This work is a result of project Move2LowC-Combustíveis de Base Biológica, with reference POCI-01-0247-FEDER-046117, cofounded by the European Regional Development Fund (ERDF), through the Operational Programme for Competitiveness and Internationalization (COMPETE2020) and the Lisbon Regional Operational Programme (LISBOA2020), under the PORTUGAL 2020 Partnership Agreement. This research was also funded by FCT/MCTES (PIDDAC): LSRE-LCM—UIDB/50020/2020 (DOI: 10.54499/UIDB/50020/2020), UIDP/50020/2020 (DOI: 10.54499/UIDP/50020/2020) and ALiCE—LA/P/0045/2020 (DOI: 10.54499/LA/P/0045/2020). K. K. Ferreira acknowledges her Ph.D. scholarship (2022.12949.BD) from FCT.

Data Availability Statement: The original contributions presented in this study are included in this article/the Supplementary Materials. Further inquiries can be directed to the corresponding author.

Acknowledgments: The authors are thankful to Universidade de Trás-os-Montes e Alto Douro (UTAD) for the XRD analyses.

Conflicts of Interest: The authors declare no conflicts of interest.

References

1. Teter, J.; Voswinkel, F. International Energy Agency 2023. Available online: https://www.iea.org/energy-system/transport (accessed on 26 April 2024).
2. Song, M.; Zhang, X.; Chen, Y.; Zhang, Q.; Chen, L.; Liu, J.; Ma, L. Hydroprocessing of Lipids: An Effective Production Process for Sustainable Aviation Fuel. *Energy* **2023**, *283*, 129107. [CrossRef]
3. Calijuri, M.L.; Silva, T.A.; Magalhães, I.B.; Pereira, A.S.A.d.P.; Marangon, B.B.; Assis, L.R.d.; Lorentz, J.F. Bioproducts from Microalgae Biomass: Technology, Sustainability, Challenges and Opportunities. *Chemosphere* **2022**, *305*, 135508. [CrossRef] [PubMed]
4. Frega, N.; Mozzon, M.; Lercker, G. Effects of Free Fatty Acids on Oxidative Stability of Vegetable Oil. *J. Am. Oil Chem. Soc.* **1999**, *76*, 325–329. [CrossRef]
5. Mba, O.I.; Dumont, M.J.; Ngadi, M. Palm Oil: Processing, Characterization and Utilization in the Food Industry—A Review. *Food Biosci.* **2015**, *10*, 26–41. [CrossRef]
6. Karatzos, S.; van Dyk, J.S.; McMillan, J.D.; Saddler, J. Drop-in Biofuel Production via Conventional (Lipid/Fatty Acid) and Advanced (Biomass) Routes. Part I. *Biofuels Bioprod. Biorefining* **2017**, *11*, 344–362. [CrossRef]
7. Kumar, M.; Olajire Oyedun, A.; Kumar, A. A Review on the Current Status of Various Hydrothermal Technologies on Biomass Feedstock. *Renew. Sustain. Energy Rev.* **2018**, *81*, 1742–1770. [CrossRef]
8. Zhang, M.; Hu, Y.; Wang, H.; Li, H.; Han, X.; Zeng, Y.; Xu, C.C. A Review of Bio-Oil Upgrading by Catalytic Hydrotreatment: Advances, Challenges, and Prospects. *Mol. Catal.* **2021**, *504*, 111438. [CrossRef]
9. Magalhães, I.B.; Pereira, A.S.A.d.P.; Silva, T.A.; Renato, N.d.S. Predicting the Higher Heating Value of Microalgae Biomass Based on Proximate and Ultimate Analysis. *Algal Res.* **2022**, *64*, 102677. [CrossRef]
10. Ding, R.; Wu, Y.; Chen, Y.; Liang, J.; Liu, J.; Yang, M. Effective Hydrodeoxygenation of Palmitic Acid to Diesel-like Hydrocarbons over MoO_2/CNTs Catalyst. *Chem. Eng. Sci.* **2015**, *135*, 517–525. [CrossRef]
11. Shi, Y.; Cao, Y.; Duan, Y.; Chen, H.; Chen, Y.; Yang, M.; Wu, Y. Upgrading of Palmitic Acid to Iso-Alkanes over Bi-Functional Mo/ZSM-22 Catalysts. *Green. Chem.* **2016**, *18*, 4633–4648. [CrossRef]
12. Cao, Y.; Shi, Y.; Bi, Y.; Wu, K.; Hu, S.; Wu, Y.; Huang, S. Hydrodeoxygenation and Hydroisomerization of Palmitic Acid over Bi-Functional Co/H-ZSM-22 Catalysts. *Fuel Process. Technol.* **2018**, *172*, 29–35. [CrossRef]
13. Feng, F.; Niu, X.; Wang, L.; Zhang, X.; Wang, Q. TEOS-Modified Ni/ZSM-5 Nanosheet Catalysts for Hydroconversion of Oleic Acid to High-Performance Aviation Fuel: Effect of Acid Spatial Distribution. *Microporous Mesoporous Mater.* **2020**, *291*, 109705. [CrossRef]
14. Khan, S.; Kay Lup, A.N.; Qureshi, K.M.; Abnisa, F.; Wan Daud, W.M.A.; Patah, M.F.A. A Review on Deoxygenation of Triglycerides for Jet Fuel Range Hydrocarbons. *J. Anal. Appl. Pyrolysis* **2019**, *140*, 1–24. [CrossRef]
15. Shi, Y.; Li, R.; Shen, Q.; Yang, M.; Wu, Y. The Selective Production of Jet Fuel Range Alkanes: Via the Catalytic Upgrading of Palmitic Acid over Co/HMCM-49 Catalysts. *Chem. Commun.* **2019**, *55*, 12096–12099. [CrossRef] [PubMed]
16. Kim, S.K.; Brand, S.; Lee, H.S.; Kim, Y.; Kim, J. Production of Renewable Diesel by Hydrotreatment of Soybean Oil: Effect of Reaction Parameters. *Chem. Eng. J.* **2013**, *228*, 114–123. [CrossRef]
17. Mäki-Arvela, P.; Martínez-Klimov, M.; Murzin, D.Y. Hydroconversion of Fatty Acids and Vegetable Oils for Production of Jet Fuels. *Fuel* **2021**, *306*, 121673. [CrossRef]
18. Sinha, A.K.; Anand, M.; Rana, B.S.; Kumar, R.; Farooqui, S.A.; Sibi, M.G.; Kumar, R.; Joshi, R.K. Development of Hydroprocessing Route to Transportation Fuels from Non-Edible Plant-Oils. *Catal. Surv. Asia* **2013**, *17*, 1–13. [CrossRef]
19. Li, X.; Lin, M.; Li, R.; Lu, Q.; Yang, M.; Wu, Y. Preparation of Metal-Acid Bifunctional Catalyst Ni/ZSM-22 for Palmitic Acid Catalytic Deoxygenation. *Fuel* **2023**, *332*. [CrossRef]

20. Georgakilas, V.; Perman, J.A.; Tucek, J.; Zboril, R. Broad Family of Carbon Nanoallotropes: Classification, Chemistry, and Applications of Fullerenes, Carbon Dots, Nanotubes, Graphene, Nanodiamonds, and Combined Superstructures. *Chem. Rev.* **2015**, *115*, 4744–4822. [CrossRef]
21. Zhong, J.; Deng, Q.; Cai, T.; Li, X.; Gao, R.; Wang, J.; Zeng, Z.; Dai, G.; Deng, S. Graphitic Carbon Embedded FeNi Nanoparticles for Efficient Deoxygenation of Stearic Acid without Using Hydrogen and Solvent. *Fuel* **2021**, *292*. [CrossRef]
22. Liu, X.; Yang, M.; Deng, Z.; Dasgupta, A.; Guo, Y. Hydrothermal Hydrodeoxygenation of Palmitic Acid over Pt/C Catalyst: Mechanism and Kinetic Modeling. *Chem. Eng. J.* **2021**, *407*. [CrossRef]
23. Lin, M.; Yan, Y.; Li, X.; Li, R.; Wu, Y. Hydrothermal Hydrogenation/Deoxygenation of Palmitic Acid to Alkanes over Ni/Activated Carbon Catalyst. *Chin. J. Chem. Eng.* **2024**, *66*, 8–18. [CrossRef]
24. Ribeiro, L.S.; Delgado, J.J.; de Melo Órfão, J.J.; Ribeiro Pereira, M.F. Influence of the Surface Chemistry of Multiwalled Carbon Nanotubes on the Selective Conversion of Cellulose into Sorbitol. *ChemCatChem* **2017**, *9*, 888–896. [CrossRef]
25. Figueiredo, J.L.; Pereira, M.F.R.; Freitas, M.M.A.; Órfão, J.J.M. Modification of the Surface Chemistry of Activated Carbons. *Carbon* **1999**, *37*, 1379–1389. [CrossRef]
26. Ding, R.; Wu, Y.; Chen, Y.; Chen, H.; Wang, J.; Shi, Y.; Yang, M. Catalytic Hydrodeoxygenation of Palmitic Acid over a Bifunctional Co-Doped MoO2/CNTs Catalyst: An Insight into the Promoting Effect of Cobalt. *Catal Sci Technol* **2016**, *6*, 2065–2076. [CrossRef]
27. Hassel, O.; Mark, H. Über Die Kristallstruktur Des Graphits. *Z. Physik* **1924**, *25*, 317–337. [CrossRef]
28. Kazakova, M.A.; Vatutina, Y.V.; Selyutin, A.G.; Prosvirin, I.P.; Gerasimov, E.Y.; Klimov, O.V.; Noskov, A.S.; Kazakov, M.O. Design of Improved CoMo Hydrotreating Catalyst via Engineering of Carbon Nanotubes@alumina Composite Support. *Appl. Catal. B* **2023**, *328*. [CrossRef]